Measurement Tool for Dynamics of Soil Cracks

Ryan D. Stewart[1*], Majdi R. Abou Najm[1,2,3], David E. Rupp[4,5], John S. Selker[1]

[1] *Biological & Ecological Engineering Department, Oregon State University, Corvallis, OR, USA.*

[2] *Civil & Environmental Engineering, Massachusetts Institute of Technology. Cambridge, MA, USA*

[3] *Now at Civil & Environmental Engineering, American University of Beirut, Beirut, Lebanon*

[4] *Cooperative Institute for Marine Resources Studies, Oregon State University, Newport, OR, USA.*

[5] *Now at Oregon Climate Change Research Institute, College of Oceanic and Atmospheric Sciences, Oregon State University, Corvallis, OR, USA*

*Corresponding author (stewarry@onid.orst.edu)

Measurement Tool for Dynamics of Soil Cracks

Abstract

Shrinkage cracks in soil function as a dominant control on the partitioning and distribution of moisture fluxes in the vadose zone. Their dynamics influence moisture balance and control water availability for runoff, deep infiltration, and near-surface storage. We present a new low-cost field instrument to monitor the temporal change in crack volume as affected by shrinkage and swelling cycles. The proposed *crack-o-meter* is composed of a sealed impermeable bag connected by a hose to a standpipe. An automated level logger records changes in water level in the standpipe, which correspond to volumetric changes of the crack. Results from two laboratory experiments show that the volume change observed by the *crack-o-meter* instruments scales linearly with the actual volume change, with an average error of 3%. The instrument was then used in a field experiment in Chile, where it measured the closing of cracks due to soil swelling.

Introduction

Expansive clay soils are characterized by spatially and temporally dynamic crack networks, which function as dominant controls on the partitioning of surface and subsurface water fluxes within expansive soils. The presence of a crack network can increase infiltration rates and allow for faster and deeper percolation of water and solutes (e.g. Messing and Jarvis, 1990; Bronswijk *et al.*, 1995; Greve *et al.*, 2010), while also enhancing soil moisture evaporation rates (Weisbrod et al., 2009). As a result, crack networks affect surface, soil, and ground water quantity and quality.

Capturing the dynamic nature of crack networks has been a theoretical and experimental challenge that has impacted our understanding of water movement in soils at the pedon, field, hillslope, and watershed scales. Numerous studies have attempted to characterize landscape-scale cracking behavior (e.g. Bronswijk, 1988; Arnold *et al.*, 2005), but up to the present, field methods have been mostly limited to estimating the instantaneous volume or the shape of a crack. In addition, many of the methods have the drawbacks of being destructive, being based only on surface characteristics, or being so labor-intensive that taking multiple measurements over a period of time can be impractical, particularly during the faster wetting phase. Examples of destructive methods include sand filling (Dasog and Shashidhara, 1993); serial sectioning of soil (Lightart et al., 1993); pouring liquid latex (Abou Najm et al., 2010); and coupling spray techniques of different dye tracers (Lu and Wu, 2003; Kasteel et al., 2005) with various image analysis methods (Aeby et al., 1997; Forrer et al., 2000; Bogner et al., 2008) for visualization of preferential flow paths. Surface-based methods to monitor crack evolution include surface image analysis (Flowers and Lal, 1999; Abou Najm, 2009); observing soil's

natural foaming (Mitchell and van Genuchten, 1993); and soil surface elevation monitoring (Wells et al., 2003; Arnold et al., 2005), which can be used to estimate the evolution of the crack network by assuming isotropy of shrinkage. Examples of labor intensive methods include a variety of crack tracing techniques utilizing thin flexible metal probes for depth detection and simple geometric assumption for volume estimation (Zein El Abedine and Robinson, 1971; Ringrose-Voase and Sanidad, 1996; Deeks et al., 1999; Bhushan and Sharma, 2002; Bandyopadhyay et al., 2003; Kishné et al., 2009) and calipers for measuring crack geometry (Návar et al., 2002).

In this technical note, we propose the *crack-o-meter* as a novel instrument for measuring transient crack-volume in the field. This instrument is simple to construct, low-cost, non-destructive, requires minimal effort to install or maintain, and allows for temporal and spatial measurements of volume changes for individual cracks. By having all these characteristics, this instrument overcomes many of the drawbacks of the aforementioned techniques. The instrument uses a sealed plastic bag connected by a hose to a polyvinyl chloride (PVC) standpipe which contains a water level logger. Laboratory and field experiments validated the design.

Method

An empty water-impermeable bag is placed into an existing crack and water is added via a standpipe until the bag has expanded to the boundaries of the crack and the water level within the standpipe has equilibrated above the hose connection (Figure 1). An automated pressure logger is placed at the bottom of the standpipe to continuously measure the pressure head inside the standpipe (p_{water}). In applications where sealed (non-

differential) pressure transducers are used, an additional pressure transducer or nearby weather station is needed to correct for barometric pressure ($p_{barometric}$) fluctuations. Water column height (h_{water}) is found by $h_{water} = (p_{water} - p_{barometric})/(g\rho_{water})$.

To reduce trapped air bubbles in the system, the bag should be free of air during insertion into the soil and the water should be introduced to the pipe slowly. Orienting the bag so that the hose is at the uppermost position can help eliminate air bubbles. At the surface, the bag can also be manually adjusted after filling to force bubbles from the system, assuming care is taken to minimize impact on crack structure.

As the crack shrinks or swells, its volume changes; this causes the water-filled bag to shrink or expand equally, which in turn causes an equivalent displacement of water volume in the standpipe. This change in water level in the standpipe (Δh) is measured and converted to volumetric change (ΔV), using $\Delta V = \pi r^2 \Delta h$, where r is the internal radius of the standpipe.

This setup was tested in a controlled laboratory experiment at Oregon State University (43°33’59”N, 123°16’50”W) in Corvallis, Oregon, and at field site in the Chilean commune of Ninhue (36°25’04”S, 72°31’05”W). Onset Corporation HOBO U20-001 (0-9 m ± 0.005 m) pressure transducers were used to monitor water level within the standpipes. An additional U20 logger was used to record barometric pressure at the field site (for barometric pressure correction), while the laboratory experiment used barometric data from the National Climatic Data Center weather station at the Corvallis airport (KCVO).

Laboratory Experiment

For the controlled laboratory experiment, a 0.55 x 0.42 x 0.25 m (55 liter) plastic storage bin was filled with Witham clay, a soil of basaltic origin, composed of approximately 55% clay, 40% silt and 5% sand (Soil Survey Staff, 2011). The soil was sieved while at field-saturated water content (using a 4 mm screen) and compacted using 100 strikes per layer with a 4.5 cm diameter, 1,880 g mini-sledge hammer. The hammer was hand-held and struck against the soil with moderate force. Final soil column height was approximately 0.16 m. The soil was allowed to air dry for six weeks until a large shrinkage crack formed near the center, at which point the water-impermeable bag – a 1000 mL Injection IV bag (B. Braun Medical Inc.) – was installed. The IV bag was connected to a 0.0254 m (inner diameter) PVC standpipe via 0.0064 m (inner diameter) plastic tubing.

The effective length (L) of the IV injection bag was approximately 0.26 m, while the bag was inserted into the crack to an approximate depth (D) of 0.082 m. Thus, assuming that the crack is V-shaped, the change in average crack width (ΔW) can be approximated using Equation 1:

$$\Delta W = 2\Delta V / LD \qquad (1)$$

where ΔV is the volume displacement measured by the instrument, L is the effective (water-filled) length of the bag, and D is the inserted depth of the bag.

After the instrument was installed, the soil was rewetted by blowing air with atomized water droplets (provided by a Vick's-brand vaporizing humidifier) with an application rate of approximately 1 L day^{-1} (equivalent to 0.0043 m day^{-1} of water) and by a direct application of 0.0025 m day^{-1} of water to the soil surface.

Another laboratory experiment was used to assess the measurement error of the proposed *crack-o-meter*. An artificial triangular shaped crack (Figure 2.a) was made from two 0.6 x 0.2 m pieces of 5/8" (0.016 m) plywood, joined at one edge by two door hinges. The artificial crack was put into a bench vise, and the *crack-o-meter* was installed covering a space confined between W_{top} and W_{bottom} (Figure 2.a), using the same instrument configuration as in the previous experiment. The objective of this second experiment was to estimate the measurement error from this *crack-o-meter* configuration.

The vice was closed in quarter-turn increments until a minimum volume was obtained, and then was reopened in quarter-turn increments until the crack was at its initial opening width. At each step, the actual dimensions (W_{top} and W_{bottom}) for crack width were measured across the bottom and top of the IV bag (as shown in Figure 2.a). Actual crack volume corresponding to the space sampled by the *crack-o-meter* instrument was calculated by $V_{actual} = ½(W_{top} + W_{bottom}) \times D \times L$, where D is the effective depth and L is the effective length of the IV bag. For this configuration D = 0.11 m and L = 0.26 m. Measured crack volume was calculated from water level in the standpipe using the same procedure as in the previous experiment.

For this experiment, the percent volume change, *V*(%), was calculated as percentage of the range between the maximum (V_{max}) and minimum (V_{min}) measured crack volumes (simulating maximum shrinkage and swelling, respectively) :

$$V(\%) = 100 \times \frac{V_{\max} - V_i}{V_{\max} - V_{\min}} \qquad (2)$$

where V_i is the measured crack volume at each measured increment.

Field Experiment

Three *crack-o-meter* instruments were placed in an active research site in the Chilean Eighth Region. The instruments were installed on January 16th and 17th, 2011, within a single 3.5 by 11 m irrigation plot. The irrigation plot was orientated so that the long dimension was approximately in the direction of highest gradient (i.e., downslope). Installation #1 was located approximately 3 meters from the upslope edge of the plot. Installations #2 and #3 were located at approximately the center of the plot, as shown in Figure 1. The IV injection bags were inserted vertically into the cracks, reaching an average maximum depth of 0.22 m from the surface. The PVC standpipes had inner diameters of 0.0285 m. Figure 1 shows the irrigation plot, from the upslope, left corner, facing downhill. The soil was classified as clay, made up of approximately 30% sand, 20% silt, and 50% clay.

The plot was irrigated with four 90-minute applications over a two-day period (January 17th and 18th, 2011), with a total cumulative application of approximately 0.17 m of water. Soil moisture content was monitored with Decagon 5TM soil moisture probes at 0.15, 0.30, 0.60 and 0.85 m depths. Runoff from the irrigation experiments was captured into collection barrels to allow for calculation of runoff rates and volumes.

Results and Discussions

Laboratory Experiments

Results from the initial controlled laboratory experiment showed that during one month of active wetting of the soil within the plastic container, Δh_{water} in the standpipe changed by 0.28 m, which corresponds to a volumetric change (ΔV) of 1.4 x 10^{-4} m^3 (Figure 3).

159 The trend was monotonic, with some noise which was inherent to the barometric
160 correction of the pressure readings. Approximately 70% of the total volume change
161 occurred in the first week. Overhead photographs confirm that by the end of the
162 experiment the crack had changed in width from approximately 0.025 m to 0.012 m, due
163 to soil swelling (Figure 3). Figure 3 presents good agreement between actual (accurately
164 measured from digital image analysis) and measured (using *crack-o-meter*) crack widths,
165 with average error of 3%.

166 Similarly, the simulated crack experiment showed that the relative volume change, as
167 measured by the *crack-o-meter* instrument, scaled linearly with the actual crack volume
168 (Figure 2.b), with no observed directional hysteresis. This configuration of the *crack-o-*
169 *meter* showed promising results, with an average error of 3% and a maximum error of 6%
170 between actual and measured volume change. However, it should be noted that this error
171 is only specific to this particular configuration and pressure sensor; different bag
172 geometries, standpipe configurations and measurement devices would have different (and
173 potentially smaller) magnitudes of intrinsic error.

174 *Field Experiment*

175 Figure 4 shows changes in crack volume for Installations #1 and #2 (the results of
176 Installation #3 are not included due to instrument malfunction). In general, the field data
177 showed significant changes in crack volume as a result of simulated rainfall. Most of the
178 swelling occurred during the four irrigation events, though some swelling continued in
179 the hours between the irrigations (Figure 4.b). The near surface (0.10 – 0.30 m) water
180 content increased quickly following the first irrigation, from nearly dry conditions (26%

181 average volumetric water content) to near saturation (about 50% average volumetric
182 water content) (Figure 4.c). The break between the first two irrigations allowed some
183 water to percolate, thus decreasing the water content of the upper soil to about 45%. This
184 redistribution process did not reverse the swelling, as can be seen by comparing Figures
185 4.b and 4.c.

186 Similarly, the overnight break between the second and third irrigations allowed for some
187 redistribution of water, during which time the water content of the upper soil again
188 decreased from about 50% to 45%, yet the swelling process did not reverse. On the
189 contrary, the swelling continued perceptibly, after irrigation stopped, for about 3 hours at
190 Installation #2 and for about 12 hours at Installation #1.

191 Finally, the soil saturated quickly after the third irrigation and stayed at a steady 50%
192 water content, with no further redistribution observed. The soil showed notable swelling
193 during the third and fourth irrigation events; little change in crack volume was observed
194 during the last hours of observation following the fourth irrigation.

195 The field results indicate that crack closure can become temporally decoupled from bulk
196 soil moisture. Assuming that the observed changes in crack volumes are primarily due to
197 changes in crack width, the temporal trends seen in Installations #1 and #2 are consistent
198 with the results of Návar et al. (2002), who measured crack dimensions during and after
199 simulated rainfall events, and observed that the majority of the cracks demonstrated
200 significant closure during the first hour of irrigation (up to 50% decrease in width), but
201 that complete closure did not happen for three more months (until 0.450 m of cumulative
202 rainfall had been applied).

Installation and Modeling Considerations

Initial results under controlled laboratory (Figures 2 and 3) and uncontrolled field (Figure 4) conditions demonstrated the capability of the proposed *crack-o-meter* instrument to monitor the relative changes in crack volumes through time. These measurements of temporal crack dynamics, coupled with field observations, can provide valuable inputs to existing shrinkage and crack-pattern models. Such models provide predictions of total volume change and degree of shrinkage isotropy (e.g. Bronswijk, 1988, using the shrinkage curve and an estimated geometry factor, r_s), crack depth and spacing of primary cracks (e.g. Konrad and Ayad, 1997), and surface crack patterns (e.g. Vogel *et al.*, 2005). Likewise, these results may be used to calibrate and validate hydrological models that accommodate macropore dynamics (e.g. Jarvis *et al.*, 1991; Greco, 2002), by comparing measured relative crack volumes to those calculated based on soil matrix water content and potential.

Care should be taken when extending (scaling-up) the results from the local experiment to the entire field. For example, the *crack-o-meter* instrument only samples a portion of the crack volume due to the fixed geometry of the impermeable bag (as seen in Figure 2.a). This can be of particular concern when shrinkage is not isotropic, such as in very dry soils where crack width has reached a maximum but crack depth continues to increase (Zein el Abedine and Robinson, 1971). Furthermore, the limited flexibility of the impermeable bags means that the instrument may be unable capture fine-scale volumetric changes when cracks possess rough, angled and/or blocky surfaces. At the same time, a sampling bias can occur because these instruments can only be installed in larger shrinkage cracks (those of at least 1 cm width). While large cracks have been shown to

preferentially transport water and solutes (e.g. Messing and Jarvis, 1990; Greve *et al.*, 2010), Bronswijk *et al.* (1995) found that small, intra-aggregate cracks also contributed significantly to solute transport.

One way to improve the accuracy of the method is through proper selection of representative crack spacing and crack shape models, given field-specific conditions. For example, with respect to crack-shape models, we have assumed V-shaped (triangular) crack cross-sectional geometries. While this is a commonly assumed cross-sectional geometry (e.g., Zein el Abedine and Robinson, 1971; Elias, *et al.*, 2001), other studies have proposed that cracks are rectangular, with parallel walls (e.g. Scott *et al.*, 1986; Dasog and Shashidhara, 1993). In addition, Ringrose-Voase and Sanidad (1996) concluded that rectangular geometries are most likely to be found in wide, mature cracks (no longer shrinking horizontally), whereas the triangular shape is likely more valid for horizontally-evolving cracks. Therefore, assuming a cross-sectional shape based on the knowledge of crack's surface conditions may help limit error in total crack volume estimates.

Finally, there was some concern that the pressure head of the water within a vertical standpipe will provide resistance to the swelling soil. In our current configuration, the water column can reach a maximum height of approximately 1.5 m (which corresponds to 15 kPa). Laboratory experiments on swelling pressures of expansive clay soils show swelling pressures which range from 200 – 1200 kPa (Basma *et al.*, 1995). Therefore, even on the low end of swelling pressures the resistance due to the water column should be minor. At the same time, future modifications to the design, such as non-vertical standpipes (to lessen the pressure head acting against the soil), specially-manufactured

bags (which can be made more flexible and in different geometries), and alternative methods of measuring the water displacement (such as weighing the mass displaced or using optical measurements) can help to both limit pressure impacts on the soil structure and to improve the overall accuracy of the instrument.

Altogether, attention to installation details, coupled with proper understanding of field cracking patterns, can help improve the accuracy of the method and eliminate potential sources of error. Nonetheless, as shown by the initial results (Figures 2, 3 and 4), even in its current configuration the instrument is able to accurately capture the initial and intermediate stages of crack closure.

Conclusion

We present a practical "*crack-o-meter*", which can be used to quantify the temporal changes in the volume of individual cracks, as demonstrated by laboratory and field experiments. All successful installations showed that swelling occurs shortly after the soil is wetted. Furthermore, we observed continued swelling at the field site for hours after water application had ceased, even when the local bulk soil moisture content slightly declined. This highlights that (1) there is a temporal component to soil swelling, and that (2) bulk soil volume is not a one-to-one function with bulk water content.

Finally, although the current experimental design allowed for the installation of only one *crack-o-meter* instrument per crack, it is conceivable that multiple instruments or bag compartments, connected to individual standpipes, could be used at multiple depths or spatial locations within a single crack. Such use of different configurations and orientations may lead to insight on the manner in which shrinkage cracks open and close,

which can have important implications for modeling hydrologic response and vadose zone transport.

Acknowledgements

This material is based upon work supported by the National Science Foundation (NSF) under Grant No. 0943682. The authors would like to acknowledge Dr. Hamil Uribe and the Chilean Instituto Nacional de Investigaciones Agropecuarias (INIA) for providing collaboration and field site support. Furthermore, the authors would like to acknowledge the participants of the NSF-funded Undergraduate Chilean Field Hydrology Course for assisting with field installation and data collection: Zak Grimes, Hayden Ausland, Mackenzie Osypian, Alex Fisher, Jennifer Vettel, Julianne Quinn, Jenna Duffin, William Rhoads, Hazel Owens, Leah Kammel, Rachel Gross, Daniela Castañeda, Liam Kyle Cahill, Maria Brown, Nick Dummer, Chuan Li, Wiebke Boettche, Felipe Bretón, Sebastián Bonelli, Hector Flores, Ghislaine Rossel, Claudia Maureira, and Marianela Matta. Finally, the authors would like to extend their gratitude to José Luis Arumí and Diego Rivera of the Department of Recursos Hídricos at the Universidad de Concepción, Chillán, for providing logistical support.

References

Abou Najm, M. R. 2009. Soil water interaction: Lessons across scales. Ph.D. dissertation. Purdue Univ., West Lafayette, Indiana.

Abou Najm, M., J. D. Jabro, W. M. Iversen, R. H. Mohtar, and R. G. Evans. 2010. New method for the characterization of three-dimensional preferential flow paths in the field. Water Resour. Res. 46, W02503. doi:10.1029/2009WR008594.

Abu-Hejleh, A.N., and D. Znidarcic. 1995. Desiccation theory for soft cohesive soils. J. Geotech. Eng.–ASCE. 121(6):493–502.

Aeby, P., J. Forrer, C. Steinmeier, and H. Fluhler. 1997. Image analysis for determination of dye tracer concentrations in sand columns. Soil Sci. Soc. Am. J. 61:33–35.

Arnold, J. G., K. N. Potter, K. W. King, and P. M Allen. 2005. Estimation of soil cracking and the effect on surface runoff in a Texas Blackland Prairie watershed. Hydrol. Process. 19:589–603. doi:10.1002/hyp.5609.

Bandyopadhyay, K., M. Mohanty, D. Painuli, A. Misra, K. Hati, K. Mandal, P. Ghosh, R. Chaudhary, and C. Acharya. 2003. Influence of tillage practices and nutrient management on crack parameters in a vertisol of central India. Soil Tillage Res. 71:133–142.

Basma, A. A., A .S. Al-Homoud, and A. Husein. 1995. Laboratory assessment of swelling pressure of expansive soils. Appl. Clay Sci. 9(5):355–368.

307 Bhushan, L., and P. Sharma. 2002. Long term effects of lantana (Lantana spp. L.) residue
308 additions on soil physical properties under rice-wheat cropping: Part I. Soil
309 consistency, surface cracking and clod formation. Soil Tillage Res. 65:157–167.
310 doi:10.1016/S0167-1987(01)00279-3.

311 Bogner, C., B. Wolf, M. Schlather, and B. Huwe. 2008. Analyzing flow patterns from
312 dye tracer experiments in forest soil using extreme value statistics. Eur. J. Soil
313 Sci. 59:103–113.

314 Bronswijk, J. 1988. Modeling of water balance, cracking and subsidence of clay soils. J.
315 Hydrol. 97:199–212.

316 Bronswijk, J., W. Hamminga, and K. Oostindie. 1995. Field-Scale Solute Transport in a
317 Heavy Clay Soil. Water Resour. Res. 31(3):517–526.

318 Dasog, G., and G. Shashidhara. 1993. Dimension and volume of cracks in a vertisol
319 under different crop covers. Soil Sci. 156(6):424–428. doi:10.1097/00010694-
320 199312000-00007.

321 Deeks, L., A. Williams, J. Dowd, and D. Scholefield. 1999. Quantification of pore size
322 distribution and the movement of solutes through isolated soil blocks. Geoderma.
323 90:65–86. doi:10.1016/S0016-7061(98)00092-5.

324 Elias, E. A., A. A. Salih, and F. Alaily. 2001. Cracking patterns in the Vertisols of the
325 Sudan Gezira at the end of dry season. Int. Agrophysics. 15:151–155.

326 Flowers, M., and R. Lal. 1999. Axle load and tillage effects on the shrinkage
327 characteristics of Mollic Ochraqualf in northwest Ohio. Soil Tillage Res. 50:251–
328 258. doi:10.1016/S0167-1987(99)00009-4.

329 Forrer, I., A. Papritz, R. Kasteel, H. Fluhler, and D. Luca. 2000. Quantifying dye tracers
330 in soil profiles by image processing. Eur. J. Soil Sci. 51:313–322.
331 doi:10.1046/j.1365-2389.2000.00315.x.

332 Greco, R. 2002. Preferential flow in macroporous swelling soil with internal catchment:
333 model development and applications. J. Hydrol. 269:150–168.

334 Greve, A.K., M.S. Andersen, and R.I. Acworth. 2010. Investigations of soil cracking and
335 preferential flow in a weighing lysimeter filled with cracking clay soil. J. Hydrol.
336 393(1-2):105–113.

337 Jarvis, N. J., P.-E. Jansson, P. E. Dik, and I. Messing. 1991. Modelling water and solute
338 transport in macroporous soil. I. Model description and sensitivity analysis. J. Soil
339 Sci. 42:59–70.

340 Kasteel, R., M. Burkhardt, S. Giesa, and H. Vereecken. 2005. Characterization of field
341 tracer transport using high-resolution images. Vadose Zone J. 4:101–111.
342 doi:10.2113/4.1.101.

343 Kishné, A. Sz., C.L. Morgan, and W.L. Miller. 2009. Vertisol crack formation associated
344 with gilgai and soil moisture in the Texas Gulf Coast Prairie. Soil Sci. Soc. Am. J.
345 73:1221–1230.

346 Konrad, J.-M., and R. Ayad. 1997. An idealized framework for the analysis of cohesive
347 soils undergoing desiccation. Can. Geotech. J. 34:477–488.

348 Lightart, T., G. Peek, and E. Taber. 1993. A method for the three dimensional mapping of
349 earthworm burrow systems. Geoderma. 57:129–141. doi:10.1016/0016-7061(93)
350 90151-A.

351 Lu, J., and L. Wu. 2003. Visualizing bromide and iodide water tracer in soil profiles by
352 spray methods. J. Environ. Qual. 32:363–367.

353 Messing, I. and N. J. Jarvis. 1990. Seasonal variation in field-saturated hydraulic
354 conductivity in two swelling clay soils in Sweden. J. Soil Sci. 41:229-237.

355 Mitchell, A., and M. van Genuchten. 1993. Flood irrigation of a cracked soil. Soil Sci.
356 Soc. Am. J. 57:490–497.

357 Návar, J., J. Mendez, R.B. Bryan, and N.J. Kuhn. 2002. The contribution of shrinkage
358 cracks to bypass flow during simulated and natural rainfall experiments in
359 northeastern Mexico. Can. J. Soil Sci. 82:65–74.

360 Ringrose-Voase, A., and W. Sanidad. 1996. A method for measuring the development of
361 surface cracks in soils: Application to crack development after lowland rice.
362 Geoderma. 71:245–261. doi:10.1016/0016-7061(96) 00008-0.

363 Scott, G.J., R. Webster and S. Nortcliff. 1986. An analysis of crack pattern in clay soil: its
364 density and orientation. J. Soil Sci. 37:653–668.

365 Soil Survey Staff. Natural Resources Conservation Service. United States Department of
366 Agriculture. Web Soil Survey. Available online at http://websoilsurvey.nrcs.
367 usda.gov/ Accessed 04/18/2011.

368 Vogel, H.-J., H. Hoffmann, A. Leopold, and K. Roth. 2005. Studies of crack dynamics in
369 clay soil: II. A physically based model for crack formation. Geoderma. 125(3–
370 4)213–223.

371 Weisbrod, N., M. I. Dragila, U. Nachshon, and M. Pillersdorf. 2009. Falling through the
372 cracks: The role of fractures in Earth-atmosphere gas exchange. Geophys. Res.
373 Lett. 36. L02401. doi:10.1029/2008GL036096.

374 Wells, R. R., D.A. DiCarlo, T.S. Steenhuis, J.-Y. Parlange, M.J. Römkens, and S.N.
375 Prasad. 2003. Infiltration and Surface Geometry Features of a Swelling Soil
376 following Successive Simulated Rainstorms. Soil Sci. Soc. Am. J. 67:1344–1351.

377 Zein El Abedine, A. and G. Robinson. 1971. A study on cracking in some Vertisols of the
378 Sudan. Geoderma. 5:229–241.

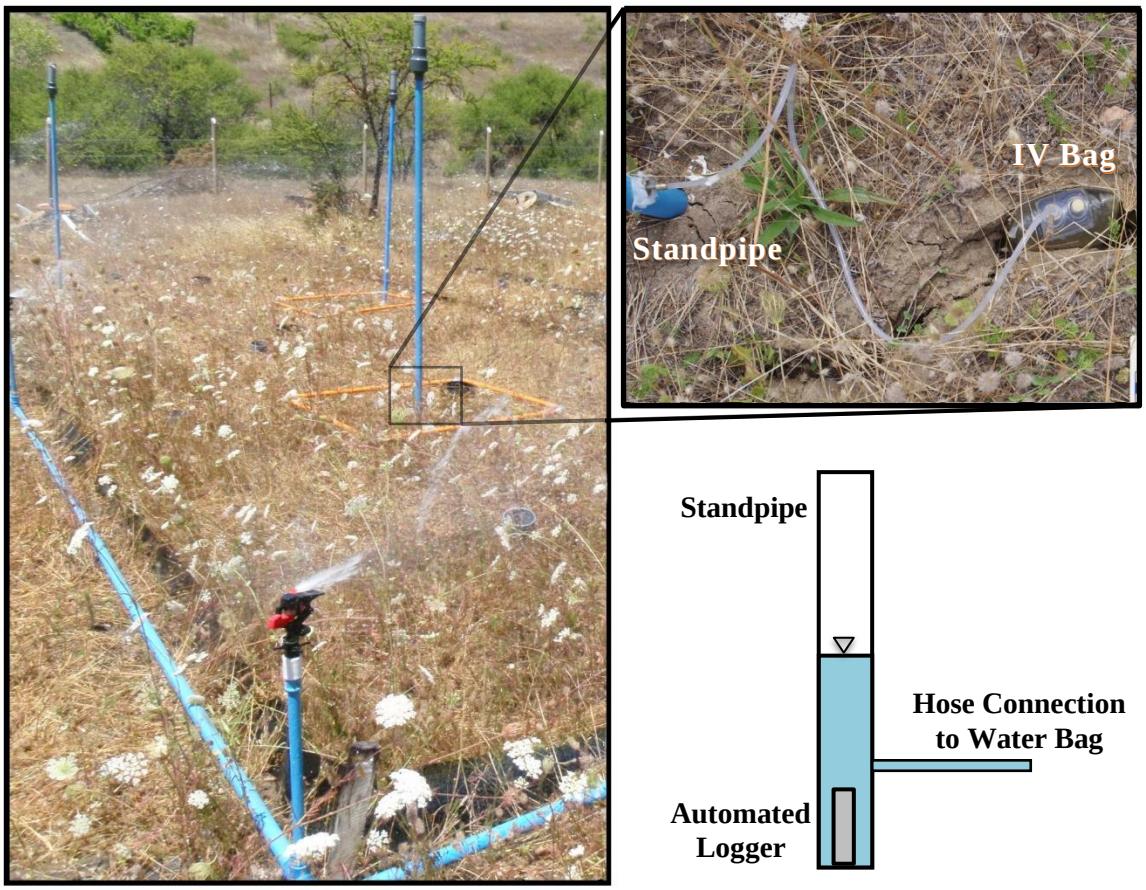

Figure 1: Schematic of the *crack-o-meter* with field images showing the installations and the details of the setup. Installation #1 is located closest to the camera; Installation #2 is in the top left corner of the image; and Installation #3 is in the middle. Notes: The orange squares surrounding Installations #1 and #3 are frames for digital crack monitoring. The sprinkler in operation at foreground is part of the rainfall/runoff simulation irrigation system. The attachments on top of the standpipes provided housing for a secondary water level measurement sensor (which failed to function properly during this experiment).

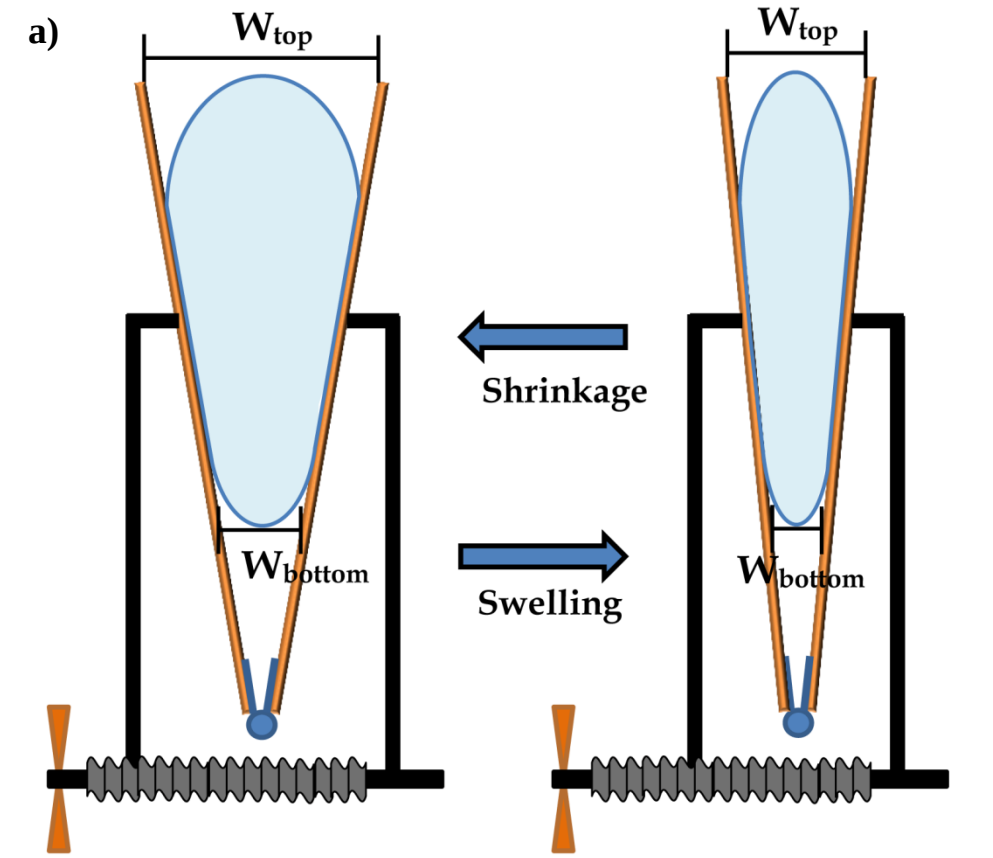
a)
W_{top}
W_{bottom}
Shrinkage
Swelling
W_{top}
W_{bottom}

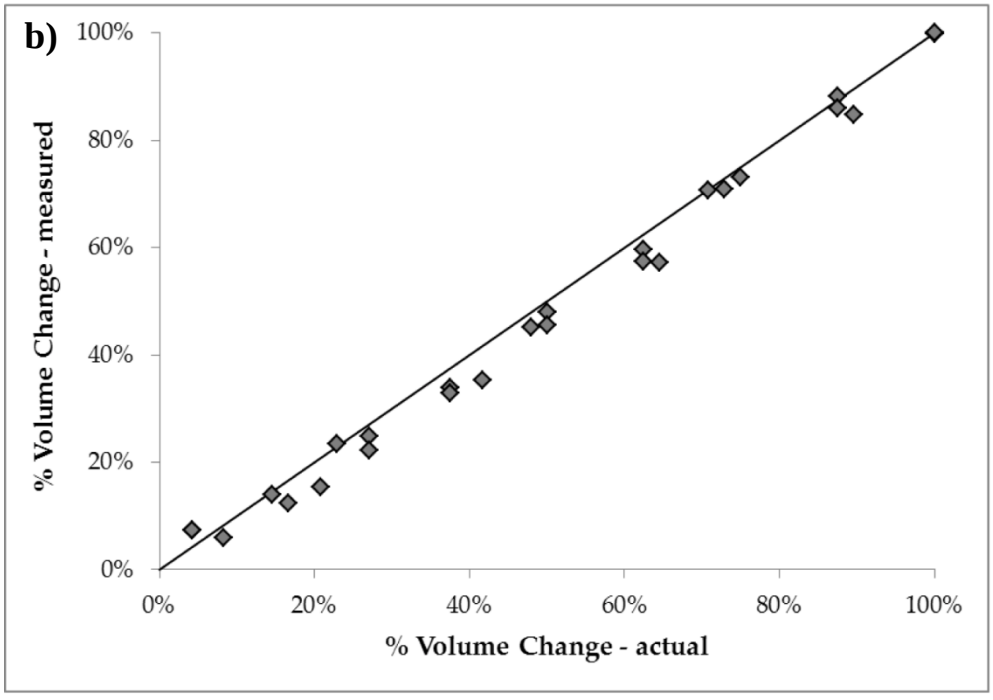
b)
100%
80%
60%
40%
20%
0%
% Volume Change - measured
0%
20%
40%
60%
80%
100%
% Volume Change - actual

388

Figure 2: (a) Schematic of the laboratory experiment used to quantify *crack-o-meter* instrument error for the current instrument configuration; (b) Percent change in volume based on a simulated triangular crack. Average error was 3% and maximum error was 6%.

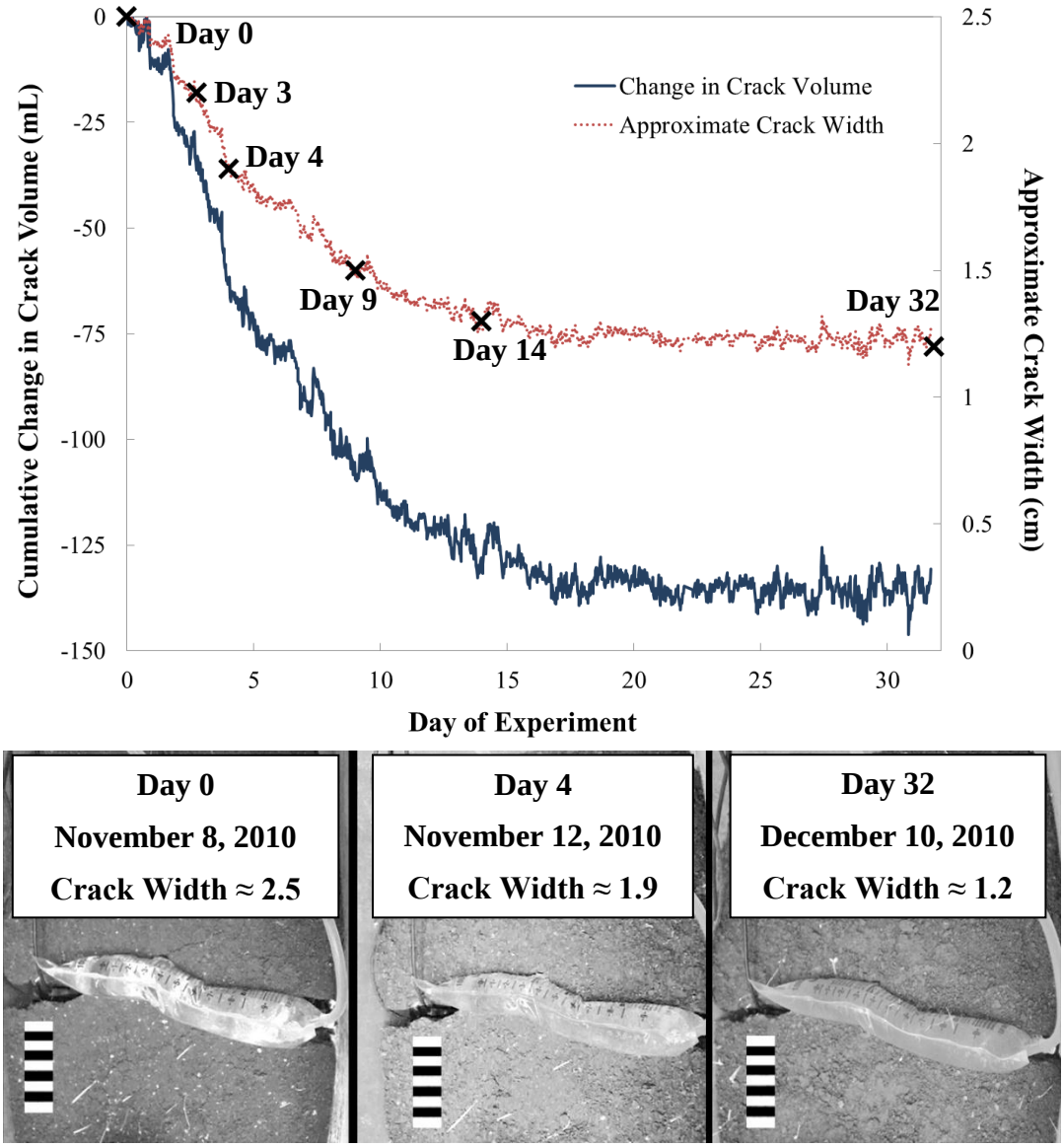

393

394 **Figure 3: Total change in crack volume, and corresponding crack width, as**
395 **measured by the laboratory *crack-o-meter* instrument. Day 0 corresponds to**
396 **November 8th, 2010. The points marked with X's correspond to the validation points**
397 **from the digital images shown in the lower part of the Figure (Note that the images**
398 **from Days 3, 9 and 32 are not shown). The reference scale shows 1 cm increments.**

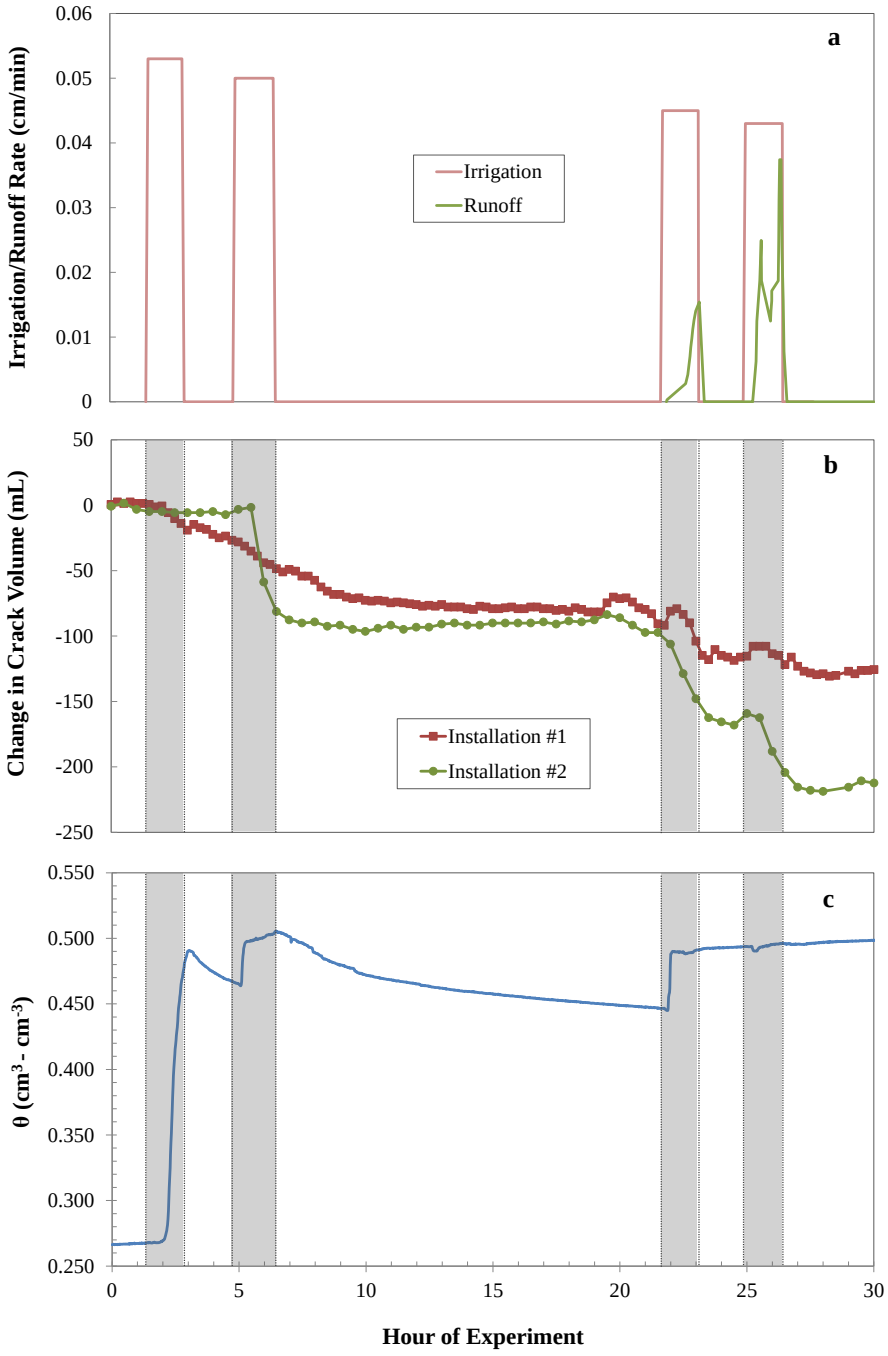

399

400 **Figure 4: (a) The four irrigation-runoff experiments showing the volume and timing**
401 **of irrigation and runoff; (b) Cumulative change in crack volumes as the result of 4**
402 **rainfall simulation events; and (c) average near surface (0.1 – 0.3 m) soil moisture.**
403 **Time = 0 corresponds to 12:00:00 PM on January 17, 2011.**